

**This paper was published in Optics Letters and is made available as an electronic reprint with the permission of OSA. The paper can be found at the following URL on the OSA website: <http://dx.doi.org/10.1364/OL.35.001392>. Systematic or multiple reproduction or distribution to multiple locations via electronic or other means is prohibited and is subject to penalties under law.**

# High-quality fiber-optic polarization entanglement distribution at 1.3 $\mu\text{m}$ telecom wavelength

Tian Zhong,<sup>1,3,†</sup> Xiaolong Hu,<sup>1,4,†</sup> Franco N. C. Wong,<sup>1</sup> Karl K. Berggren,<sup>1</sup>  
Tony D. Roberts,<sup>2</sup> and Philip Battle<sup>2</sup>

<sup>1</sup>Research Laboratory of Electronics, Massachusetts Institute of Technology, Cambridge, Massachusetts 02139, USA

<sup>2</sup>AdvR, Inc., 2310 University Way, Building #1, Bozeman, Montana 59715, USA

<sup>3</sup>tzhong@mit.edu

<sup>4</sup>xlhu@mit.edu

Received January 6, 2010; revised March 11, 2010; accepted March 15, 2010;  
posted March 23, 2010 (Doc. ID 122285); published April 26, 2010

We demonstrate high-quality distribution of 1.3  $\mu\text{m}$  polarization-entangled photons generated from a fiber-coupled periodically poled  $\text{KTiOPO}_4$  waveguide over 200 m fiber-optic cables. Time-multiplexed measurements with a 19% efficient superconducting nanowire single-photon detector at the remote location show a detected flux of 5.8 pairs/s at a pump power of 25  $\mu\text{W}$  and an average two-photon quantum-interference visibility of 97.7% without subtraction of accidentals. © 2010 Optical Society of America

OCIS codes: 270.5585, 030.5260, 060.5565.

Many proof-of-principle experiments in quantum information science have been performed primarily with polarization-entangled photons in the near-IR region (700–900 nm), where efficient Si single-photon counters are commercially available. However, photons at this spectral range do not propagate over long distances in standard fibers. The capability to distribute entanglement to remote locations is highly desirable. Of particular interest is an entanglement-based quantum communication system at the 1.3  $\mu\text{m}$  telecom band, which would allow the quantum network to coexist with the standard 1.55  $\mu\text{m}$  telecom fiber-optic infrastructure with minimal effects owing to cross talk and nonlinear spurious signals.

Robust fiber-based entanglement distribution requires efficient generation and detection of high-quality entangled photons at telecom wavelengths, and the decoherence characteristics of the fiber network must be taken into account, especially for polarization-entangled photons. Polarization entanglement generation in a bulk nonlinear crystal is not well suited for fiber-optic distribution because of inefficient coupling of the multispatial mode output into a single-mode fiber. The coupling problem is eliminated in fiber sources, but liquid-nitrogen cooling is often required to suppress significant background noise owing to Raman scattering [1]. In addition, detection with InGaAs avalanche photodiode (APD) single-photon counters can be problematic owing to high dark-count rates relative to Si APD counters. In this Letter we present a high-visibility 1.3  $\mu\text{m}$  polarization entanglement source based on a fiber-coupled nonlinear waveguide and coincidence detection by a high-efficiency superconducting nanowire single-photon detector (SNSPD) without subtraction of accidental coincidences. The source-detector combination enables reliable distribution of polarization-entangled photons over two unattended 200 m fibers with minimal degradation over a 30 min period.

Previous waveguide-based polarization entanglement sources [2,3] have shown much lower visibilities than the 99% level obtainable in bulk-crystal sources [4]. The low visibilities are related to excessive fluorescence in near-IR waveguide sources [5] and substantial accidental coincidences caused by multipair generation and by high dark-count rates of InGaAs APD counters [2]. To achieve high visibility, we have recently developed a high-performance photon pair waveguide source with a high pair generation efficiency and, more importantly, a very low fluorescence noise of only  $\sim 2\%$  of downconverted photons within the 1.1 nm phase-matching bandwidth centered at 1316 nm [6].

Figure 1 shows the schematic of our experimental setup. We pumped the 1.6-cm-long fiber-coupled Type II phase-matched periodically poled  $\text{KTiOPO}_4$  (PP-KTP) waveguide with a cw laser diode at 658.1 nm to generate horizontally ( $H$ ) polarized signal and vertically ( $V$ ) polarized idler at 1316.2 nm for a waveguide temperature of 26.5°C. The waveguide had integrated input and output polarization-maintaining (PM) fibers with a waveguide-to-fiber coupling efficiency of  $\sim 45\%$ . Spectral indistinguishability was ensured with a free-space, pump-blocking reflection Bragg grating (RBG) filter with an FWHM bandwidth of 0.7 nm that was slightly smaller than the phase-matching bandwidth. Taking into account the spectral shape and the 90% peak transmission, the effective efficiency of the RBG filter was 75%. A 98% efficient long-pass filter further removed any residual pump power. The signal and idler were then separated by a polarizing beam splitter (PBS), coupled into their respective SMF-28 fibers, and recombined at a 50:50 fiber nonpolarizing beam splitter (NPBS). The signal and idler remained orthogonally polarized at the NPBS inputs by use of a polarization controller (PC1) in the idler arm. By considering only those events with one photon in each of the two output channels (labeled 1 and 2), we were able to generate postselectively the polarization-entangled triplet

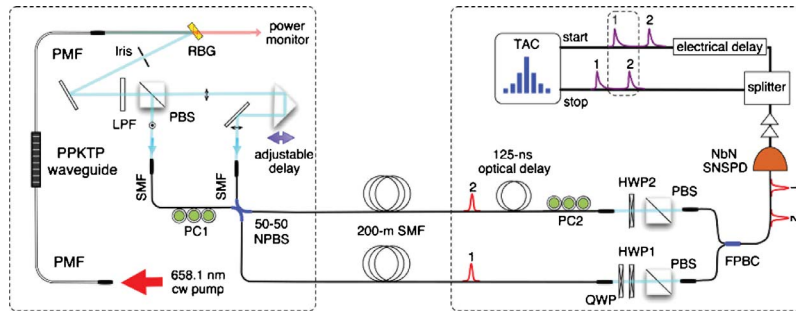


Fig. 1. (Color online) Schematic of experimental setup. PMF, polarization-maintaining fiber; SMF, single-mode fiber; RBG, reflection Bragg grating; LPF, long-pass filter; PBS, polarizing beam splitter; NPBS, nonpolarizing beam splitter; PC, polarization controller; HWP, half-wave plate; QWP, quarter-wave plate; FPBC, fiber polarizing beam combiner; TAC, time-amplitude converter.

state  $|\Phi\rangle = (|H\rangle_1|V\rangle_2 + |V\rangle_1|H\rangle_2) / \sqrt{2}$  [7]. An adjustable signal delay line after the PBS provided the necessary timing compensation to erase the temporal distinguishability caused by dispersion in the waveguide.

For detection we employed a fiber-coupled NbN SNSPD with a 19% detection efficiency (including single-mode fiber coupling) for optimal polarization at 1316 nm and a dark-count rate of  $\sim 150$  counts/s for a detector bias set at 95% of its critical current [8]. The waveguide source and the SNSPD were located in two separate buildings, and Fig. 1 shows that the entangled photons in channels 1 and 2 were sent to the SNSPD system in two separate 200-m-long SMF-28 fibers. We compensated the depolarization induced by the fiber transmission and maintained linear polarizations at the detector location by using a quarter-wave plate in channel 1 and a polarization controller (PC2) in channel 2. Polarization analysis was performed using a half-wave plate (HWP) and a PBS in each channel.

A time-multiplexed scheme was used to permit a single SNSPD to perform two-photon coincidence measurements. We imposed a time delay of 125 ns for photon 2 relative to photon 1 before they were combined at a fiber polarizing beam combiner and subsequently sent to the fiber-coupled SNSPD. The SNSPD voltage-pulse outputs were amplified by rf amplifiers and split into a “stop” channel and a “start” channel with a fixed electrical delay for time-correlated coincidence counting (1 ns coincidence window) using a time-amplitude converter (Picoquant TimeHarp200). The transmission efficiency of each fiber channel was 75%, and each of the two free-space-to-fiber coupling stages was 65% efficient. We estimate an overall system detection efficiency of  $\sim 1.43\%$  ( $\sim 0.65\%$ ) for channel 1 (2), with the difference due to polarization sensitivity of the SNSPD.

Postselective generation of polarization-entangled photons using a 50:50 beam splitter requires that the two photons be spatially, spectrally, and temporally indistinguishable, as characterized by a Hong–Ou–Mandel (HOM) interference measurement [9]. By adjusting PC1 in Fig. 1 such that the signal and idler polarizations were equal at the inputs to the fiber NPBS, we measured the HOM interference at a pump power of  $25 \mu\text{W}$  with negligible multipair gen-

eration probability within the coincidence window [5]. Figure 2 shows the measurement results taken without subtraction of accidental coincidences, yielding an HOM visibility  $V_{\text{HOM}} = (C_{\text{max}} - C_{\text{min}}) / (C_{\text{max}} + C_{\text{min}}) = 99.2\%$ , where  $C_{\text{max}}$  ( $C_{\text{min}}$ ) is the maximum (minimum) coincidence count. To the best of our knowledge, this is the highest HOM visibility reported for waveguide-based photon-pair sources. Compared with our previous measurements using gated InGaAs detectors [6], the coincidence rate per unit power has been improved by a factor of 150 owing mostly to the use of the high-efficiency SNSPD in free-running mode. More importantly, the combination of low fluorescence from the waveguide source and low dark counts of the SNSPD substantially reduced accidental coincidences to  $\sim 0.3\%$  of  $C_{\text{max}}$ , thus enabling more accurate visibility measurements without accidentals subtraction.

For polarization, entanglement generation, the signal time delay was set at the HOM dip minimum to ensure temporal indistinguishability. We characterized the entanglement distribution quality by measuring the two-photon quantum interference without subtraction of accidentals at the source and detector locations for a pump power of  $25 \mu\text{W}$ . Before fiber distribution, we placed the polarization analyzers at the source location and measured a quantum-interference visibility of 98.3% in the  $H$ - $V$  basis and 97.2% in the antidiagonal-diagonal ( $A$ - $D$ ) basis. Figure 3 displays the two-photon interference at the detector location, measuring a visibility of 98.2% and 97.2% in the  $H$ - $V$  and  $A$ - $D$  bases, respectively, and

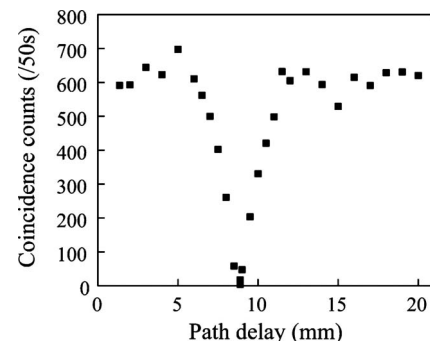


Fig. 2. Measured HOM coincidences without subtraction of accidentals as a function of the signal arm path delay at  $25 \mu\text{W}$  pump power in the PPKTP waveguide.

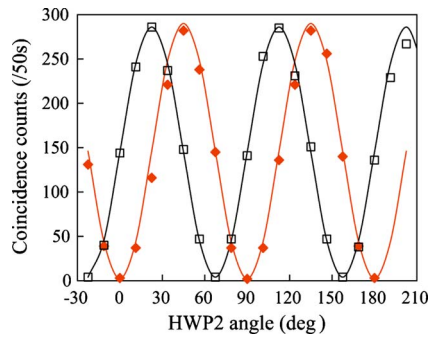


Fig. 3. (Color online) Two-photon quantum interference of distributed polarization-entangled photons in the  $H$ - $V$  basis (filled diamonds) and the  $A$ - $D$  basis (open squares) at  $25 \mu\text{W}$  pump power with no subtraction of accidentals. Solid curves are sinusoidal fits.

showing no degradation over the short fibers. Figure 4 shows the measured visibility at different pump powers, normalized to pair generation rate in the waveguide per 1 ns coincidence window  $\alpha$  (0.025% at  $25 \mu\text{W}$  pump). Visibility degrades owing to multipair events in accordance with calculation:  $V=1-2\alpha$ , for small  $\alpha$ . At very small  $\alpha$  two factors prevented the visibilities from being even higher. One is the 0.3% residual accidental coincidences. Second, a 1% visibility loss was observed owing to signal and idler channel cross talk that was caused by insufficient polarization extinction (25 dB) in the PM fiber and by axis alignment mismatch between the PM fiber and the PPKTP crystal.

Polarization entanglement may decohere in fiber propagation owing to depolarization mechanisms such as temperature fluctuation and mechanical vibration. To investigate the distributed entanglement quality over time, we repeatedly measured the two-photon quantum-interference visibility in both  $H$ - $V$  and  $A$ - $D$  bases over a duration of 150 min. The results are shown in Fig. 5, in which the time origin refers to the point when the polarizations were set correctly and the system was left unattended thereafter. We found that a visibility greater than 97% could be maintained for  $\sim 30$  min without active polarization control. For very long fiber lengths, one can use time-bin qubits for transmission and convert them to polarization qubits at the destination [10].

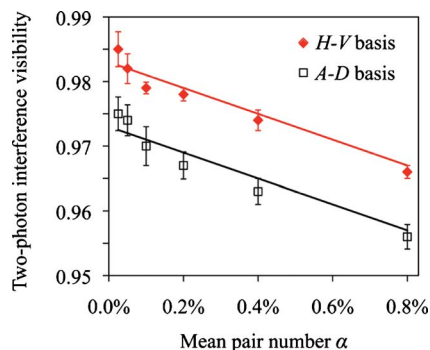


Fig. 4. (Color online) Two-photon interference visibilities (accidentals subtracted) versus  $\alpha$ . Visibilities degradation follows  $1-2\alpha$  functional dependence (solid lines) owing to multipair events.

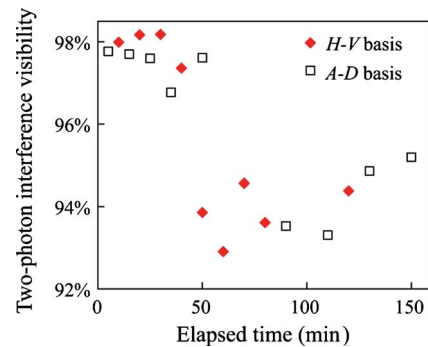


Fig. 5. (Color online) Time evolution of two-photon interference visibility in the  $H$ - $V$  (filled diamonds) and  $A$ - $D$  (open squares) bases for distributed polarization entanglement over two 200 m unattended fibers.

In summary, we have demonstrated high-quality polarization-entanglement distribution over two short-length telecom fibers, facilitated by entanglement generation using a fiber-coupled, low-noise PPKTP waveguide source and time-multiplexed coincidence detection with a single high-efficiency low-dark-count-rate SNSPD. We obtained a two-photon quantum-interference visibility of over 97% without subtraction of accidentals and showed it to be stable for  $\sim 30$  min. Our system may find applications in short-distance fiber-optic distribution of polarization entanglement, for instance, in networking between photonic and atomic qubit systems.

We thank G. N. Gol'tsman and B. Voronov for supplying the unpatterned NbN film on sapphire substrate, E. A. Dauler for technical assistance and F. Marsili for helpful discussions. This work was supported in part by IARPA through the Department of Interior contract NBCHC060071 at Massachusetts Institute of Technology and contract NBCHC060049 at AdvR.

<sup>†</sup>The authors contributed equally to this Letter.

## References

1. X. Li, P. L. Voss, J. E. Sharping, and P. Kumar, *Phys. Rev. Lett.* **94**, 053601 (2005).
2. Y.-K. Jiang and A. Tomita, *Opt. Commun.* **267**, 278 (2006).
3. A. Martin, V. Cristofori, P. Aboussouan, H. Herrmann, W. Sohler, D. B. Ostrowsky, O. Alibart, and S. Tanzilli, *Opt. Express* **17**, 1033 (2009).
4. F. N. C. Wong, J. H. Shapiro, and T. Kim, *Laser Phys.* **16**, 1517 (2006).
5. A. B. U'Ren, C. Silberhorn, K. Banaszek, and I. A. Walmsley, *Phys. Rev. Lett.* **93**, 093601 (2004).
6. T. Zhong, F. N. C. Wong, T. D. Roberts, and P. Battle, *Opt. Express* **17**, 12019 (2009).
7. C. E. Kuklewicz, M. Fiorentino, G. Messin, F. N. C. Wong, and J. H. Shapiro, *Phys. Rev. A* **69**, 013807 (2004).
8. X. Hu, T. Zhong, J. E. White, E. A. Dauler, F. Najafi, C. H. Herder, F. N. C. Wong, and K. K. Berggren, *Opt. Lett.* **34**, 3607 (2009).
9. C. K. Hong, Z. Y. Ou, and L. Mandel, *Phys. Rev. Lett.* **59**, 2044 (1987).
10. F. Bussières, J. A. Slater, J. Jin, N. Godbout, and W. Tittel, arXiv:1003.0432 (2010).